A Simple Model of Nonisothermal Coextrusion

M. E. NORDBERG III* *and* H. H. WINTER

Goessmann Laboratory
Department of Chemical Engineering
University of Massachusetts
Amherst, Massachusetts 01003

A numerical method has been developed that takes the streamline finite difference method for modeling fully developed multilayer polymer flows and adds to it a simple means of accounting for nonisothermal conditions. In industrial practice, temperature control is often used to match material viscosities and, thereby, to avoid flow instabilities. By numerically calculating both viscosity ratios and normal stress difference ratios, the numerical method allows one to judge the relative stability of different flows and to choose an intelligent set of experiments when designing a coextrusion process. The algorithm has been successfully tested for a number of polymer melt constitutive equations in flows where the viscosity jumps no more than two orders of magnitude between fluids. Results for a rheologically well characterized polystyrene low-density polyethylene system and for an industrially interesting high-density polyethylene/Ultem system show that the common practice of matching zero-shear viscosities is overly simplistic when interface shear rate, conduction, normal stress, and flow rate effects are taken into account.

INTRODUCTION

Given the importance of coextrusion in industrial practice and the use of nonisothermal conditions in coextrusion, one can identify the need for a simple procedure for modeling nonisothermal flows of polymer melts. This problem's difficulty lies in the coupling of velocity, stress, and temperature fields in a flow channel. Solutions of the problem would find application in die design (pressure drops, flow rates, etc.), in analyzing multilayer flow experiments, and in process design (particularly for temperature control of viscosity).

A number of researchers have modeled the nonisothermal flow of single polymer melts (1–7). Fewer have considered multilayer nonisothermal flows (8–10). The purpose of this work is to model nonisothermal die flows in approximately fully developed geometries.

In industrial practice, the reason for adjusting temperatures of different layers in a coextrusion process is to try to avoid instabilities in the flow by matching the viscosities of different materials. These instabilities take three forms, as illustrated in *Fig. 1*: waviness in the interface similar to melt fracture except that it occurs inside the material (11); nonuniform cross sections in, for example, a sheet coextrusion; and complete rearrangement of the two materials in a more complex extrusion (12–14). The rearrangement of the materials is driven by a mismatch in viscosities; if a surrounding material is thicker (in the sense of viscosity) than the material it surrounds, the flow could achieve a lower pressure gradient by rearranging. Another factor now being considered by researchers (15–17) is the effect of normal stress difference jumps at the interface. In this work, we make no direct predictions about stability, but by using the results of the numerical procedure illustrated here, one can say something about the relative stability of two comparable flows or one could employ empirical rules that predict when instabilities will occur in a given flow (18, 19). Numerical calculations for a desired coextrusion could suggest a set of experiments to run looking for appropriate processing conditions for the flow.

GOVERNING EQUATIONS

Four equations govern the (approximately) unidirectional nonisothermal flow of polymeric materials. These are the continuity equation, written in integral form,

$$\psi(y) = \int_0^y v\, dy; \tag{1}$$

the Cauchy equation of motion,

$$\frac{d\tau_{xy}}{dy} = \frac{dp}{dx}; \tag{2}$$

the energy equation (here written in two-dimensional

* Present address: KMS Fusion, Inc., 700 KMS Place, P.O. Box 1567, Ann Arbor, MI 48106-1567.

Interface Waviness

Nonuniform Sheet

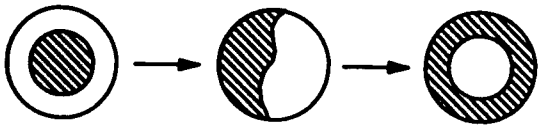

Layer Rearrangement

Fig. 1. Schematic of different types of instability in coextrusion.

form, later approximated in one-dimensional form),

$$Gz\, v \frac{dT}{dx} = \nabla^2 T + Na\, \underline{\tau} : \nabla \underline{v}; \tag{3}$$

and a constitutive equation for stress from kinematics and temperature,

$$\tau_{xy} = \eta(\dot{\gamma}, T)\dot{\gamma}; \; \dot{\gamma} = \frac{dv}{dy}. \tag{4}$$

All of the variables shown above are dimensionless, normalized by the average velocity, $\bar{v}$, the channel width, $\bar{y}$, and the viscosity at the characteristic shear rate and reference temperature, $\bar{\eta}(\bar{v}/\bar{x}, \bar{T}^0)$. The temperature is normalized by difference:

$$T = \frac{\tilde{T} - \bar{T}^0}{\Delta \bar{T}^0}, \tag{5}$$

where the reference temperature difference comes from the temperature dependence of viscosity through the shift factor, a_T:

$$[\Delta \bar{T}^0]^{-1} = -\left.\frac{\partial a_T}{\partial \tilde{T}}\right|_{\bar{T}^0}. \tag{6}$$

The shift factor may be calculated by either of two equations. The first is an Arrhenius type relation (20):

$$\ln a_T(\tilde{T}) = \frac{\bar{E}}{\bar{R}}\left[\frac{1}{\tilde{T}} - \frac{1}{\bar{T}^0}\right]. \tag{7}$$

The second is the WLF equation (21),

$$\log a_T(\tilde{T}) = \frac{-\bar{C}_1(\tilde{T} - \bar{T}^0)}{\bar{C}_2 + (\tilde{T} - \bar{T}^0)}. \tag{8}$$

Temperature coefficients of viscosity may be calculated from either of these two equations. For the Arrhenius and WLF equations, respectively, they are

$$(\Delta \bar{T}^0)^{-1} = \frac{\bar{E}}{\bar{R}(\bar{T}^0)^2}, \tag{9}$$

and

$$(\Delta \bar{T}^0)^{-1} = 2.303\, \frac{\bar{C}_1}{\bar{C}_2}. \tag{10}$$

Note that for both the Arrhenius and WLF equations, $\Delta \bar{T}^0$ is a function of the reference temperature. The Arrhenius $\Delta \bar{T}^0$ depends explicitly on $\bar{T}^0$ and the WLF coefficients $\bar{C}_1$ and $\bar{C}_2$ are implicitly functions of T^0.

The Graetz number, which appeared in the energy equation, relates the relative magnitude of convection and conduction:

$$Gz = \frac{\bar{\rho}^0\, \bar{c}_p\, \bar{v}\, \bar{x}}{\bar{k}}. \tag{11}$$

The Nahme number compares viscous dissipation with conduction:

$$Na = \frac{\bar{\rho}^0\, \bar{v}^2}{\bar{k}\, \Delta \bar{T}^0}. \tag{12}$$

The temperature and viscosity have different scalings for different materials, so fluid-fluid interface boundary conditions must account for the change in scaling. Following are the interface boundary conditions for the three conservation equations. Wall boundary conditions are traditional isothermal, nonslip conditions.

$$v_A = v_B \tag{13}$$

$$(\bar{\eta}_A/\bar{\eta}_B)\tau_{xy,A} = \tau_{xy,B} \tag{14}$$

$$\psi_A = \psi_B = \psi^* \tag{15}$$

(I.e. the flow rate of each layer is specified.)

$$\tilde{T}_A = \tilde{T}_B \tag{16}$$

$$\tilde{q}_A = \tilde{q}_B \tag{17}$$

We have not specified a constitutive equation yet; for the numerical method that follows a particular equation is not required. However, we have made use of the Wagner model (22) with Osaki strain functional (23) for this work:

$$\eta(\dot{\gamma}) = \sum_{i=1}^{m} \sum_{j=1}^{2} \frac{f_j\, g_i\, \lambda_i}{(1 + n_j\, \lambda_i\, |\dot{\gamma}|)^2}. \tag{18}$$

All material parameters in the above equations are determined by fitting experimental data. The normal stress does not enter into the solution of the governing equations. We therefore solve for the velocity first and then determine the first normal stress coefficient:

$$\Psi_1(\dot{\gamma}) = \sum_{i=1}^{m} \sum_{j=1}^{2} \frac{2 f_j\, g_i\, \lambda_i^2}{(1 + n_j\, \lambda_i\, |\dot{\gamma}|)^3}. \tag{19}$$

ADIABATIC MULTILAYER FLOWS

Nordberg and Winter (24) developed a methodology for modeling fully developed slit or annulus flows using a streamline finite difference method. All of the examples that they considered were isothermal. However, the method can be applied without major modifications for nonisothermal flows by allowing the viscosity to be a function of temperature as well as of shear rate, $\eta = \eta(T, \dot{\gamma})$. The simplest approach to account for nonisothermal conditions is to make each layer isothermal within itself without requiring a continuity of temperature at the interface, i.e., to make the layers adiabatic. Clearly this is a gross simplification, but it gives usable rough-cut results. Later in this work we develop an approximate but surprisingly useful method for modeling the conductive temperature equilibration that would take place between unequal layers. Adiabatic calculations may be sufficient for high flow rates with little time for conduction. They also serve as the first cut for later calculations.

Figure 2 shows a very simple example for a two-layer slit flow. The two layers are polystyrene (PS) and low-density polyethylene (LDPE) at 195°C and 180°C, respectively. Throughout this section, we are concerned with reducing the viscosity step at the interface. In practice, this is the purpose of temperature adjustment: to match viscosities of adjacent materials. We define the ratio to be greater than one for unfavorable configurations. The objective is to bring the viscosity ratio as close to one as possible since this is believed to avoid flow instabilities. The inset of *Fig. 2* shows that this can be done for this example. Having fixed the LDPE temperature at 180°C, 195°C is the PS temperature giving the best viscosity ratio. In this simple example, the interface is in a region of nearly zero shear rate and the two materials are quite similar, so stability is not really a question. Nonetheless, the approach is demonstrated.

Figure 3 illustrates a situation where a lower viscosity material (LDPE) is sandwiched (again in a slit) by the higher viscosity PS. In this case, the polystyrene temperature has been fixed at 195°C with the polyethylene temperature varied as shown. Because the LDPE viscosity is less temperature-sensitive, the viscosity ratio varies less, but again one can choose the "best" temperature for LDPE (185°C), which is the case actually plotted. Note that the result is a different pair of temperatures from the previous case; the viscosity ratio depends not simply on temperature but also on shear rate. The shear rate at the actual interface can be found only by solving the flow problem.

Even if by adjusting temperatures one succeeds in matching the viscosity at the interface, as in the example of *Fig. 3*, the corresponding normal stress difference profile (*Fig. 4*) may still have a sizable jump. A viscosity jump can be considered the driving force for instability through material rearrangement, but a normal stress difference jump can also cause instabilities. The jump is equivalent to a net tension on the interface and can (with any curvature) cause waviness in the interface in a way analogous to surface tension.

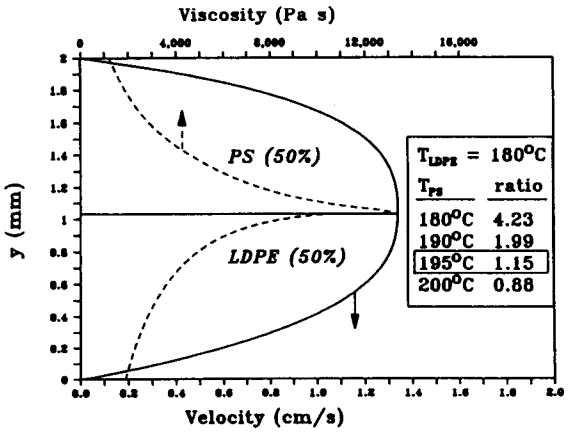

Fig. 2. Adiabatic nonisothermal sheet coextrusion of PS and LDPE. Effect of PS temperature on viscosity ratio is shown in inset.

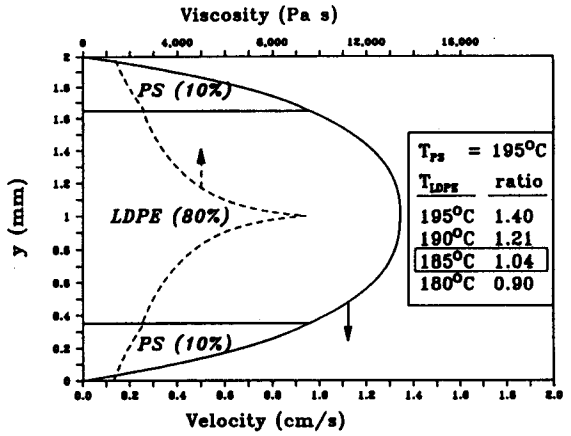

Fig. 3. Adiabatic nonisothermal sheet coextrusion of PS/LDPE/PS. Effect of LDPE temperature on viscosity ratio is shown in inset.

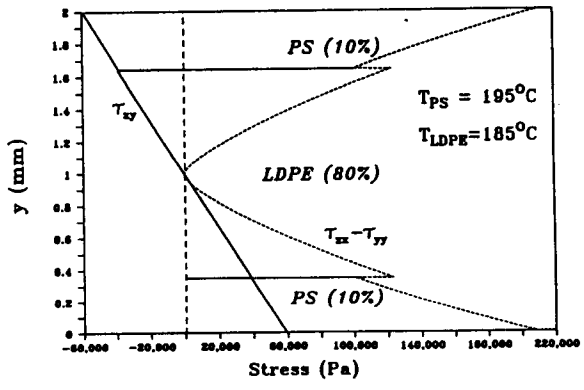

Fig. 4. Shear and normal stress difference profiles for adiabatic nonisothermal sheet coextrusion of PS/LDPE/PS.

CONDUCTIVE MULTILAYER FLOWS

Although the method of the previous paragraphs takes into account different temperatures of different materials, it makes no effort to consider the conduction between layers. The full energy equation accounts for both conduction and convection and is coupled to the equation of motion. Here, we avoid this two-dimensional problem with a method for very easily calculating an approximate temperature profile accounting for the temperature gradient between layers and a residence time t.

A simple model for the conduction between adjacent layers requires solving the following parabolic equation from the isothermal-within-layers initial condition at $t = 0$ up to $t = t_c$:

$$Gz \frac{dT}{dt} = \frac{d^2T}{dy^2}. \tag{20}$$

This equation comes from the full energy equation when one assumes plug flow for purposes of solving the energy equation. This means ignoring the viscous dissipation term of the energy equation and the cross-channel variation of the convection term. The time t is now just an overall residence or flow time. The value t_c is a "contact time," some time representative of how long the materials are allowed to contact. The solution is the same as if the layers were solid slabs initially isolated and then brought into contact for time t_c, a traditional heat transfer problem.

In this work we will assume isothermal walls, $T = T_w$, and the following equation equates conduction between layers to serve as the interface boundary condition:

$$\frac{\bar{k}_A \, \Delta\bar{T}_A^{\,0}}{\bar{k}_B \, \Delta\bar{T}_B^{\,0}} \frac{dT_A}{dy} - \frac{dT_B}{dy} = 0. \tag{21}$$

The energy equation, *Eq 20*, with boundary conditions expressed by *Eq 21* may be solved by a standard Crank-Nicolson method (25). The only detail different from the standard approach is that one must use streamline finite differences for temperature similar to those developed for velocity and viscosity in Nordberg and Winter (24). Another implementation detail is that the temperature is normalized differently in each layer, so careful bookkeeping is necessary for grid points neighboring an interface. This is done in a way similar to the appearance of $\Delta\bar{T}_A^{\,0}/\Delta\bar{T}_B^{\,0}$ in *Eq 21*, which comes from the different scalings of temperature in the different fluids.

The numerical method defined by this approximation is as follows:

- —Using isothermal conditions within each layer, solve for the kinematics.
- —Fixing the layer geometry at the values just calculated, allow conduction between layers for a period t_c.
- —Recalculate the kinematics using this new temperature profile and accounting for the temperature dependence of viscosity.

One could go further, and make this an iterative procedure, but it can be observed in practice that interface positions do not change much from the first step to the third, so iteration is unnecessary.

Figure 5 uses the method just outlined to continue the example of *Fig. 3*. In this case 185°C and 195°C are the inlet or original bulk temperatures of the LDPE and PS, but now conduction is allowed between layers for the period t_c. The effect on the viscosity ratio is shown in the inset. The profile plotted is for a reasonable value of $t_c = 0.1$ s. The effect on viscosity ratio is significant: The conduction between the layers reintroduces the original viscosity jump, making it even worse than under isothermal conditions. One can immediately conclude from this that a more accurate measure of stability in nonisothermal cases will have to account for the viscosity *field*, not simply the interface ratio. *Figure 6* compares the viscosity and temperature profiles for the cases of *Figs. 3* and *5*. Away from the interface, the effect of conduction is small, but at and near the interface it is noticeable even for very small t_c. The region affected expands with t_c. The figure explains why the viscosity ratio is

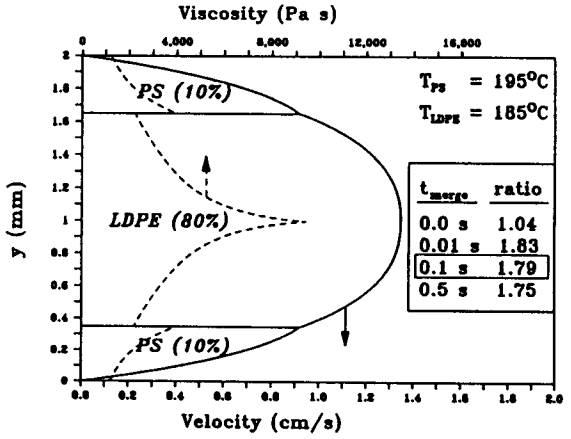

Fig. 5. Conductive nonisothermal sheet coextrusion of PS/LDPE/PS. Effect of conduction time, t_{merge}, on viscosity ratio is shown in inset.

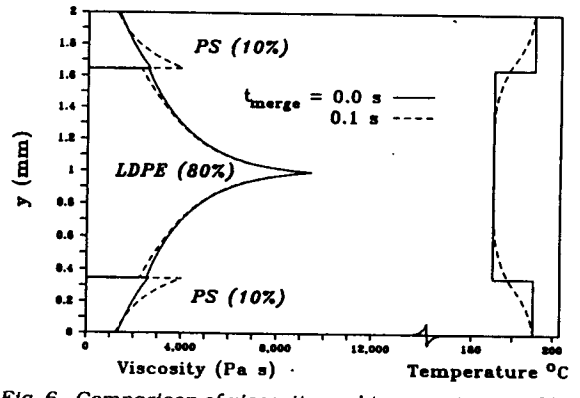

Fig. 6. Comparison of viscosity and temperature profiles for adiabatic and conductive sheet coextrusion of PS/LDPE/PS.

worse than in the isothermal base case: the viscosities of the two materials change in opposite directions from the layer-by-layer isothermal values. *Figure 6* also confirms the claim made earlier that the interface position does not change much despite the changed temperature profile.

Note that t_c may be close to the actual contact time (however that is measured), but is better thought of as a simple modeling constant that may be chosen by the user of the method. Its use should probably be in the context of a parameter sweep as done in *Fig. 5* to see not what the "actual" viscosity ratio will be but how sensitive the flow will be to conduction between layers downstream from where they combine.

Figure 7 summarizes the results for the PS/LDPE/PS example by examining both viscosity ratios and normal stress difference ratios at the interface of this flow. Ideally one would like both ratios close to one. The base case of 195°C isothermal flow is somewhat away from this ideal, so it is instructive to consider the effects of various variables on the two ratios. Dropping the LDPE temperature drops the viscosity ratio moderately. Increasing the PS temperature has a larger effect (per °C of change) because, as shown in *Fig. 8*, PS is more temperature-sensitive than LDPE. Increasing the flow rate (i.e., $\bar{v}$) has the desirable and somewhat surprising effect of improving both the viscosity ratio and normal stress difference ratio. This is because (as again shown by *Fig. 8*) PS is more shear-thinning than LDPE; increasing the flow rate (and, therefore, the interface shear rate) drops the PS viscosity faster than the LDPE viscosity. Finally, *Fig. 7* demonstrates that the effect of conduction is to make thing worse initially, though they then slowly improve with time. Although the behavior of the PS/LDPE/PS system is rather tame, one could imagine for a more practical example expanding upon the diagram of *Fig. 7* to propose a design for a coextrusion system, or at least an intelligent set of processing experiments to run.

This type of parameter sweep we now do in detail for a more practical case. *Figure 9* illustrates the

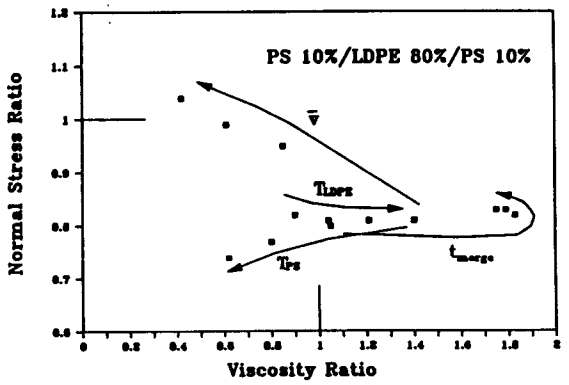

Fig. 7. Normal stress ratio vs. viscosity ratio for PS/LDPE/PS sheet coextrusion under various conditions. By the adjustment different parameters of the flow, stability is affected in different ways.

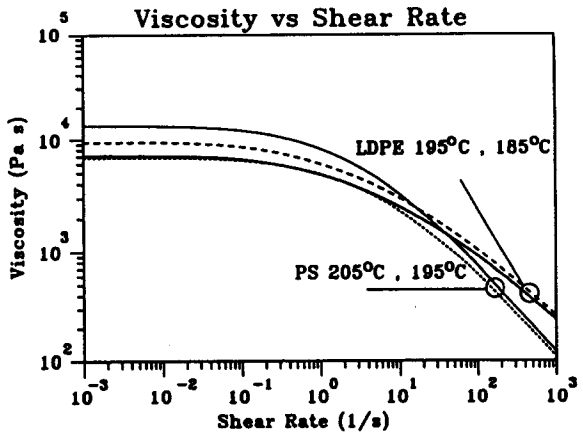

Fig. 8. Viscosity vs. shear rate and temperature for PS and LDPE (Wagner model). PS is more temperature-sensitive and more shear-thinning than LDPE.

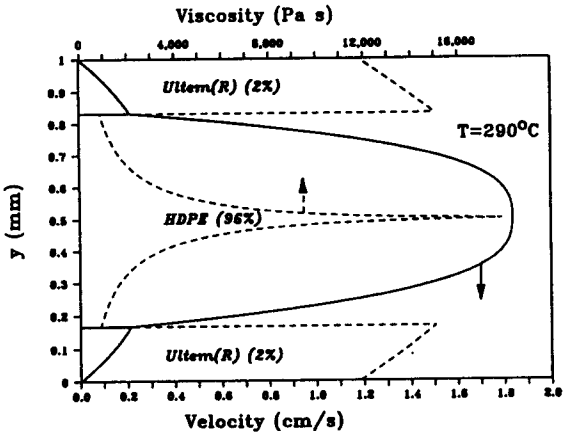

Fig. 9. Sheet coextrusion of Ultem/HDPE/Ultem. Flow is clearly unstable since the interface viscosity ratio is close to 15.

flow desired. A sheet of high-density polyethylene (HDPE) is to be extruded with a thin skin of GE's Ultem®. The extruded sheet may then be thermoformed, for example, to make microwave safe trays for food. Ultem is very heat resistant, but is also expensive. A 100% Ultem tray would be uneconomical, but a thin skin can protect the commodity HDPE without making the cost prohibitive. The difficulty illustrated in *Fig. 9* is that Ultem has a much higher viscosity than HDPE and, therefore, the desired flow configuration is unstable. In this case, the sheet typically becomes nonuniform across its width (26). An approach taken at GE Plastics was to add additional layers of HDPE to act as lubricant at the walls, as illustrated in *Fig. 10*. HDPE is incompatible with Ultem (the analysis has neglected the tie layers that must appear between the inner HDPE and the desired Ultem skin), so the extra layer may be peeled off the final product and discarded or recycled (inset of *Fig. 10*).

Table 1 begins with the base case of *Fig. 10* and varies several parameters to get an idea of the sen-

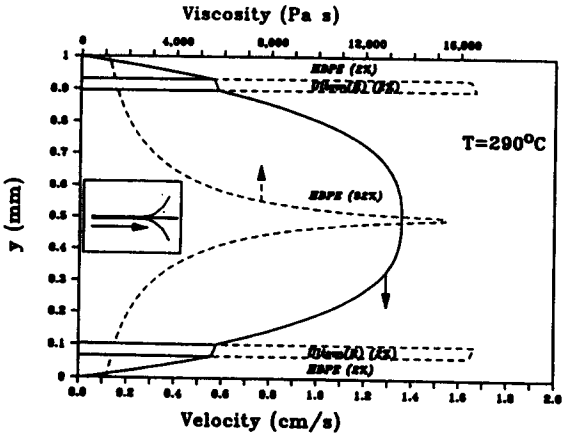

Fig. 10. Sheet coextrusion of Ultem/HDPE/Ultem with HDPE lubricant. The outer HDPE layer is peeled off outside the die. A tie layer between the core HDPE and Ultem has been neglected (also in Fig. 9).

Table 1. Parameter Sweep for HDPE/Ultem/HDPE/Ultem/HDPE Sheet Coextrusion Example.

Base Conditions			Vary Flow Rate	
			$\bar{v}$	Ratio
HDPE	2%	290°C	1 cm/s	10.9
Ultem	2%	290°C	5 cm/s	22.7
HDPE	92%	290°C	10 cm/s	29.4
Ultem	2%	290°C		
HDPE	2%	290°C		

Vary Core Temp.		Vary Skin %	
T	Ratio	%	Ratio
290°C	10.9	2%	10.9
250°C	10.0	6%	9.2
200°C	8.7	10%	8.0

Vary Ultem Temp		Vary Merge Time	
T	Ratio	t_c	Ratio
290°C	10.9	0.0 s	1.7
320°C	1.7	0.01 s	6.6
		0.1 s	9.7
		0.5 s	10.7

sitivity of the flow to each. Our measure of stability is simply the viscosity ratio at the interface between the core HDPE and Ultem layers. First one can vary the overall flow rate to learn that the flow will become noticeably less stable at higher flow rates. (This effect is more pronounced when the interface is in a high shear rate region as it is here.) Another parameter that could be adjusted is the temperature of the core HDPE. However, changing this temperature has little effect on the viscosity ratio (*Table 1*) because HDPE is not highly temperature sensitive, as may be seen in *Fig. 11*. A third parameter one can consider is the relative thickness of the outer HDPE skin. Increasing the thickness of the lubricant decreases the instability of the flow slightly. The most effective way (apparently) to increase stability in this flow is to increase the temperature of the Ultem. *Table 1*

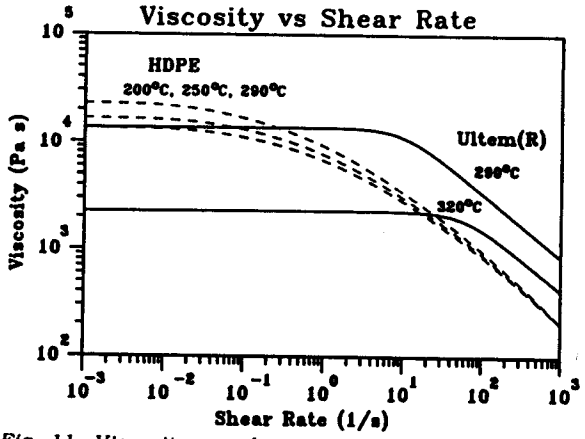

Fig. 11. Viscosity vs. shear rate and temperature for HDPE and Ultem. Ultem is much more temperature-sensitive than HDPE.

shows the viscosity ratio dropping an order of magnitude for a slight increase in Ultem temperature. This is because the Ultem is highly temperature sensitive (*Fig. 11*). The final check of *Table 1*, however, suggests that conduction from the Ultem into the HDPE would increase the ratio rapidly (because the Ultem layer is so thin). This might suggest the desirability of heating the walls to keep the outer two layers hotter than the inner core. One could also go on to consider combinations of the options studied in *Table 1*. This example illustrates how the numerical method of this section could be used as a simple design tool (or perhaps as a process "prescreening" tool) for actual coextrusion problems.

CONCLUSIONS

Nonisothermal coextrusion flows can be modeled with increasing levels of sophistication. We presented here a simple "fully developed" method for modeling such flows that takes into account the temperature profile that might be seen in nonisothermal coextrusion but does not carefully solve the two-dimensional energy equation. The objective was to empirically predict stability in such flows through two simple parameters, the viscosity ratio at the interface between fluids and the similar ratio in normal stress difference. The modeling can then be taken as a predictive tool for designing coextrusion processes.

Though this paper considers only two examples, it shows that the simplistic approach of adjusting material temperatures to match viscosities gives an insufficient understanding of the problems occurring, particularly if the matching is done via low shear rate data. First, the matching should be done at the shear rate actually present at the interface, which requires modeling of the flow, a primary incentive for this work. Second, not only viscosity but also normal stress has an influence on the stability of a fluid-fluid interface. Modeling of the type presented here allows calculation of both viscosity and normal stress ratios. And third, when conduction between layers is considered, even by the approximate method

of this article, it becomes clear that in nonisothermal flows information purely at the interface is incomplete. One would conclude from simple viscosity ratios that adjusting temperatures will in many cases actually have an adverse effect. A more detailed study of stability would have to account for material behavior in some neighborhood of the interface, perhaps through an extension of the present methods to time-dependent flows.

APPENDIX

The appendix lists the material properties of the polymers used in the modeling examples of this study.

LDPE (27)

$\bar{T}^0 = 150°C$
$\bar{\rho}^0 = 780$ kg/m^3
$\bar{E}/\bar{R} = 6{,}341$ K
$\bar{k} = 0.223$ W/m·K (28)
$\bar{C}_p = 2{,}370$ J/kg·K (28)
$n_1 = 0.304$
$n_2 = 0.07$
$f = 0.67$

g_i (Pa)	λ_i (s)
37.76	59.13
371.0	18.17
1,952	3.68
10,800	0.6606
28,060	0.1073
60,400	0.02060
137,100	0.003026
302,700	0.0003381

PS (27)

$\bar{T}^0 = 180°C$
$\bar{\rho}^0 = 970$ kg/m^3
$C_1 = 5.61$
$C_2 = 143.2$ K
$\bar{k} = 0.14$ W/m·K (28)
$\bar{C}_p \approx 1{,}000$ J/kg·K
$n_1 = 0.377$
$n_2 = 0.073$
$f = 0.88$

g_i (Pa)	λ_i (s)
77.63	51.52
1,338	8.669
927.5	5.135
17,620	1.018
50,040	0.1107
69,780	0.01065
100,900	0.0009927
555,800	0.00005821

HDPE (27)

$\bar{T}^0 = 170°C$
$\bar{\rho}^0 = 960$ kg/m^3
$\bar{E}/\bar{R} = 2{,}093$ K
$\bar{k} = 0.26$ W/m·K (28)
$\bar{C}_p = 3{,}682$ J/kg·K (28)
$n_1 = 0.447$
$n_2 = 0.098$
$f = 0.74$

g_i (Pa)	λ_i (s)
343.4	34.35
2,925	4.282
5,048	1.035
18,640	0.3082
41,800	0.04120
38,400	0.02302
156,500	0.003378
211,500	0.0005155

Ultem® (26)

$\bar{T}^0 = 290°C$
$\bar{E}/\bar{R} \approx 20{,}000$ K
$\bar{k} \approx 0.2$ W/m·K
$\bar{C}_p \approx 3{,}000$ J/kg·K

Carreau Model:

$\eta = \eta_0[1 + (\lambda\dot{\gamma})^2]^{[n-1)/2}$
$\bar{\eta}_0 \approx 18{,}000$ Pa·s
$\bar{\lambda} \approx 0.1$ s
$n \approx 0.4$

ACKNOWLEDGMENT

The authors gratefully acknowledge the support of GE Plastics, Pittsfield, Mass.

NOMENCLATURE

Notation Conventions

$\hat{x}$	=	dimensional value.
$\bar{x}$	=	reference dimensional value.
x	=	nondimensional value.

English Symbols

a_T	=	viscosity shift factor.
C_1, C_2	=	WLF equation parameters.
E	=	Arrhenius equation activation energy.
f	=	parameter (weighting) in Osaki strain functional.
g	=	individual modulus value in linear viscoelastic spectrum.
Gz	=	Graetz number.
k	=	thermal conductivity.
n	=	parameter (exponent) in Osaki strain functional.
p	=	pressure.
q	=	heat flux.
R	=	ideal gas constant.
t	=	flow time.
T	=	temperature.
v	=	velocity.
x	=	Cartesian coordinate in flow direction.
y	=	coordinate perpendicular to flow.

Greek Symbols

η	=	viscosity.
λ	=	material relaxation time constant.
ρ	=	density.
τ_{xy}	=	shear stress.
ψ	=	stream function.
Ψ_1	=	first normal stress coefficient.

Subscripts

A	=	inner material near an interface.
B	=	outer material near an interface.
c	=	contact time.

Superscripts

0	=	temperature dependent reference value.

REFERENCES

1. E. Mitsoulis, *Adv. Polym. Technol.*, 6, 467 (1986).
2. H. H. Winter, *Adv. Heat Transfer*, 13, 205 (1977).
3. B. Vergnes, P., Saillard, and J. F. Agassant, *Polym. Eng. Sci.*, 24, 980 (1984).
4. X.-L. Luo and R. I. Tanner, *J. Non-Newt. Fluid. Mech.*, 22, 61 (1986).
5. X.-L. Luo and R. I. Tanner, *Rheol. Acta*, 26, 499 (1987).
6. F. Sugeng, N. Phan-Thien, and R. I. Tanner, *J. Rheol.*, 31, 37 (1987).
7. M. A. McClelland and B. A. Finlayson, *J. Non-Newt. Fluid. Mech.*, 27, 363 (1988).
8. E. Uhland, *Polym. Eng. Sci.*, 17, 671 (1975).
9. S. Basu, *Polym. Eng. Sci.*, 21, 1128 (1981).
10. G. Sornberger, B. Vergnes, and J. F. Agassant, *Polym. Eng. Sci.*, 26, 682 (1986).
11. C. D. Han and R. Shetty, *Polym. Eng. Sci.*, 18, 180 (1978).
12. J. L. White, R. C. Ufford, K. R. Dharod, and R. L. Price, *J. Appl. Polym. Sci.*, 16, 1313 (1972).
13. A. Kariagiannis, H. Mavridis, A. N. Hrymak, and J. Vlachopoulos, *SPE ANTEC Tech. Papers* 33, 106 (1987).
14. A. Kariagiannis, H. Mavridis, A. N. Hrymak, and J. Vlachopoulos, *Int. J. Numer. Meth. Fluids*, 8, 123 (1988).
15. N. D. Waters and A. M. Keeley, *J. Non-Newt. Fluid. Mech.*, 24, 161 (1987).
16. D. M. Binding, K. Walters, J. Dheur, and M. J. Crochet, *Phil. Trans. Roy. Soc. London*, A323, 449 (1987).
17. Y. Renard, *J. Non-Newt. Fluid. Mech.*, 28, 99 (1988).
18. C. D. Han, *Multiphase Flow in Polymer Processing*, Academic Press, New York (1981).
19. W. J. Schrenk, N. L. Bradley, T. Alfrey, and H. Maack, *Polym. Eng. Sci.*, 18, 620 (1978).
20. J. D. Ferry, *Viscoelastic Properties of Polymers*, 3rd ed, J. Wiley & Sons, New York (1980).
21. M. L. Williams, R. F. Landel, and J. D. Ferry, *J. Am. Chem. Soc.*, 77, 3701 (1955).
22. D. C. Bogue and J. O. Doughty, *I. & Eng. Chem. Fundam.*, 5, 243 (1966); M. Wagner, *Rheol. Acta*, 15, 136 (1976).
23. K. Osaki, *Proc. VII Intl. Congress on Rheology*, Gotherburg, 104 (1976).
24. M. E. Nordberg III and H. H. Winter, *Polym. Eng. Sci.*, 28, 444 (1988).
25. W. H. Press, B. P. Flannery, S. A. Teukolsky, and W. T. Vetterling, *Numerical Recipes—The Art of Scientific Computing*, Cambridge University Press, Cambridge (1986).
26. W. Lashway (personal communications, 1987–1988).
27. P. R. Soskey and H. H. Winter, *J. Rheology*, 28, 625–645 (1984).
28. R. C. Armstrong and H. H. Winter, in *Heat Exchanger Data Book*, E. U. Schlunder, ed., Hemisphere, 2.5.12–1 (1981).